Multi-modal biometric recognition system based on FLSL fusion method and MDLNN classifier

[1]Ajai Kumar Gautam, [2]Rajiv Kapoor
[12]Department of Electronics & Communication Engineering, Delhi Technological University, Delhi , India
[1]ajai.gautam@gmail.com, [2]rajivkapoor@dce.ac.in

Article History: Received: 11 January 2021; Revised: 12 February 2021; Accepted: 27 March 2021; Published online: 10 May2021

Abstract: A Multi-Modal Biometrics (MMB) system incorporates information as of more than '1' biometric modality for enhancing each biometric system's performance. Numerous prevailing research methodologies focused on MMB recognition. However, the recognition system encompasses robustness, accuracy, along with recognition rate issues. This paper proposed the MMB recognition system centred on the FLSL fusion method and Modified Deep Learning Neural Network (MDLNN) classifier in order to enhance the performance. The face, ear, retina, fingerprint, and front hand image traits are considered by the proposed method. It comprised image enhancement, segmentation, Feature Extractions (FE), Feature Reduction, feature fusion, rule generation, and identification phases. The Improved Plateau Histogram Equalization (IPHE) algorithm enhances all the inputted traits. After that, Viola-Jones Algorithm (VJA) segmented the facial parts, and the Penalty and Pearson correlation-based Watershed Segmentation (PPWS) algorithm eliminates the unwanted information in the ear and finger traits and also segmented the blood vessel of the retina image. Region of Interests (ROI) calculation separates the palm region. Next, the features are extracted as of images, and then, the Kernelized Linear Discriminants Analysis (KLDA) algorithm reduces the features' dimensionalities. Next, the Features Level and Scores Level (FLSL) fusion method fuse the features. Therefore, the features' fused output is inputted to the MDLNN to classify the person as genuine or imposter. The investigational evaluation of the proposed MDLNN with the prevailing classifiers is analyzed. The proposed MDLNN centred MMB recognition system trounces the top-notch methods.

Keywords: Improved Plateau Histogram Equalization (IPHE), Viola-Jones Algorithm (VJA), Penalty and Pearson correlation-based Watershed Segmentation (PPWS), Kernelized Linear Discriminant Analysis (KLDA), Feature Level and Score Level (FLSL), and Modified Deep Learning Neural Network (MDLNN) algorithm.

1. INTRODUCTION

Biometrics could be found anywhere from unlocking of mobiles to airport border control recently. A modern system that utilizes the information of biometrics as of one person aimed at authentication along with verification is a biometric system [1]. For recognizing individuals, the technology of utilizing humans' physical along with behavioral characters is a biometrics system [2]. BR systems are utilized in multiple areas for recognition [3]. Besides different other factors namely cost, convenience, security level, memory requirements, etc, the BR system is also centered upon its verification or identification accuracy [4]. The genuine and imposters by means of uni-modal biometrics and MMB methods are recognized by this method. Different issues namely non-universality, intra-class variations, noise in input data, spoof attacks, along with distinctiveness are possessed by these uni-modal systems. Due to the user's poor interaction with the sensor, these variations take place [5]. The usage of numerous biometric modalities (i.e., the combination between two or several different biometrics data or combining between the physiological along with behavioral characteristics) within the same system is the solution for overcoming these disadvantages, which is named as a multiple biometric system [6, 7]. Thus, greater attention to MMB was given by most researchers for increasing identification performance and providing more security [8].

The inherent problems of user's inconvenience along with system inefficiency are solved by the MMB systems [9]. MMB systems can manage the issues of non-universality and can limit imposters from spoofing biometric attributes of authentic people. Thus, it could fulfill challenges [10]. Sometimes, the usage of disparate identities of the same trait rather than utilizing the details of disparate modalities is an MMB. For example, finger shape along with vein, fingerprints as well as finger knuckle point print of an individual human finger are the amalgamation of different traits, which are employed in finger multimodal authentication [11]. A biometric system centered upon the biometric attributes of the traits. The unique features are utilized for comparison along with matching which is sorted out as of the biometric data (raw) [12]. For improving performance, the features from different traits are merged together. Therefore, the main method involved in MMB is a fusion [13]. An amalgamation of disparate features of traits is the definition of multiple modal fusions [14]. This biometric system's accuracy is considerably affected by the scheme of fusion, which is effective.

Feature-level, sensor-level, Rank-Level Fusions (RLF), matching Score Level Fusions (SLF), along with decision-level fusions are the '5' modules in the MMB system through its fusion [15] [16]. Different classifiers

and predictors with the estimators are utilized for fusing the information largely after fusion and are composed of '3' types namely fusion before matching, fusion at the time of matching along with fusion after matching called, pre-mapping, midst mapping, along with post mapping respectively [17]. Further investigation of different stimulating factors namely privacy, cost, accuracy, selection of powerful biometric traits, system complexity, easy to use, etc. is performed as per the fusion outcome [18]. In the previous ten years, numerous MMB systems centered on conventional traits, namely fingerprint, and iris, are developed. Ear, palm print geometry, finger geometry, as well as retina are the few works about an MMB system. An MMB authentication system centered on the MDLNN algorithm is proposed by this research methodology for improving the recognition's accuracy and making the MMB authentication system quicker. The face, ear, retina, fingerprint, palmprint with palmprint geometry, along with finger geometry traits are integrated by the presented MMB.
This paper is categorized as: Section 2 described the top-notch methods of the multi-modal biometric. Section 3 elucidates the proposed methodology of the MMB recognition. Section 4 examined the proposed methodology's performance with the existing research technique. Section 5 completes the paper.

2. RELATED WORK

Nada Alay [20] introduced an MMB aimed at recognizing humans by biometric modes of face, iris, along with the finger vein centred upon a deep learning (DL) algorithm. For increasing training data along with reducing overfitting problems, pre-processing actions were initially executed on the images, namely resized the image utilizing the Visual Geometry Groups (VGG-16) as well as data augmentation was employed. Next, every biometric trait was given to its Convolutional Neural Networks (CNN) design. After that, feature level, along with SLF methods were utilized for fusing the '3' CNN's multi-modal models (iris, face, along with finger vein). The approach had comfortably outshined the top-notch methods as shown by the experimental outcomes. The approach's drawback was not implemented with different level fusion methods as it was inappropriate for complementary traits.
Meryem Regouid *et al.* [21] introduced an MMB system aimed at human identification and security centred on the local textures descriptors. For eradicating the redundant data, normalization along with segmentation was the pre-processing method applied to Electrocardiography (ECG), ear, and iris biometrics. After that, for extracting the significant features as of the ECG signal as well as converting the ear along with iris images to 1D signals, 1D-Local Binary Patterns (1D-LBP), Shifted-1D-LBP, along with 1D-Multi-Resolution-LBP were employed. K-Nearest Neighbours (KNN) and the Radius Basis Function (RBF) were employed for matching to categorize an unidentified user as the genuine or else the impostor. The approach had performed well with the MMB system by different classification methods as shown by the experimental outcomes. The KNN was utilized by the approach which was inappropriate for numerous data. The system's performance was degraded centred on distance calculation.
Gurjit Singh Walia *et al.* [22] presented an MMB system centred on an optimum SLF model. Iris, fingerprint, together with the finger's vein was the integrated '3' complementary biometric attributes. Gabor transform was implemented on the image and the following output was split as non-overlapping rectangle blocks. Aimed at every block, the LBP's histogram was determined and these extracted histograms were concatenated for forming feature vectors. Therefore, the authenticate person was identified by the feature's vectors given to the individual classifier. For acquiring a simultaneous solution, individual classifiers were resolved by Proportional Conflict Redistributions rules (PCR-6). The score dissemination of imposter together with the genuine class was large which results in high accuracy along with reliability for this approach as shown by the investigational results. The information was directly taken by the framework as of the input; then given onto the classifier that could affect the recognition's rate as a consequence of the noises prevalent in the inputted image.
S. Prabu *et al.* [23] specified a multimodal authentication for BR System centred on Intelligent Hybrid Fusion Techniques. Firstly, the image was pre-processed via the median filters for eliminating the noises and smoothening images. The resulting images were inputted to the Discrete Curvelet Transforms for better clarity. For feature detection, Effective linear Binary Patterns (ELBP) along with Scale-Invariant Fourier Transforms (SIFT) were employed. After that, the genuine, and the imposter were verified via the Extreme Learning Machines (ELM) classification method. The authentication system had attained higher accuracy by fusion method as demonstrated by the experiential outcomes. Because of the ELM classification technique, the method's robustness was not efficient.
Gaurav Jaswal *et al.* [24] introduced an MMB Authentication System by Palm Print, Hand Shape, along with Hand Geometry. The image (original) was altered as grey-scale at the pre-processing procedure and then, a 2D Gaussian filter was implemented for reducing the noise and other irregularities. Next, certain rotation along with illumination effects was experienced by the extracted palm's ROI samples that limited the corresponding performance. Utilizing the Speeded-Up Robust Features (SURF) descriptor, the transformed ROI images' local key-points had been taken out. Sub-pattern-centred PCA (SpPCA) and Support Vector Machine (SVM)-centred classification method was utilized for better recognition. A multimodal recognition system centred on the feature-level fusion of the normalized features of the palm print, hand shape, along with the hand geometry traits

had achieved better accuracy as exhibited in the experimental outcomes. This system was a complex process for recognizing the damaged contour parts of the traits.

K. Gunasekaran et al. [25] introduced a deep multimodal BR by the contour-let derivative weighted RLF with fingerprint, human face along with iris. The pre-processing was initially executed using the Contour-let Transform design. Then, the Local Derivative Ternary Patterns was implemented in the pre-processed attributes. The obtained coefficients were utilized for improving the feature discrimination power. The biometric matching scores as of numerous modalities were effectively combined by the multimodal features (extracted) to which the Weighted RLF was implemented. For improving the MMB system's recognition rate within the temporal domain, a DL framework was implemented. The investigational outcomes had demonstrated that the system had attained better results in MMB authentication. The approach's drawback was not efficient as the full image of traits was deemed and then the images were fused. The recognition's rate was affected since the redundant parts prevalent in the traits also were pondered.

3. PROPOSED MULTI-MODEL BIOMETRIC AUTHENTICATION

In the past decennia, one of the major domains of security systems has turned out to be Biometrics. Recently, the utilization of automated biometrics-centred personal recognition systems has turned out to be an omnipresent procedure. Nevertheless, several problems, such as illumination variation, noisy data, spoofing, pose variation, partial occlusion, and non-universality are confronted by the uni-modal biometrics, which brings about less accurateness and security. MMB identification is a propitious alternative to trounce few of these cons and for augmenting the level of security. This research method proposed an MMB authentication system centred on the MDLNN algorithm, which considers the face, ear, retina, fingerprint, palm print, the geometry of the palm together with the fingers. Initially, IPHE enhances all the inputted images. Next, the segmentation process is executed in which the VJA segments the face image, and also the PPWS eradicates the unnecessary information of the ear and finger image in addition to the blood vessels are segmented as of the retina. Additionally, the ROI calculation separates the palm region as of the front hand image. As of every trait, the features are extracted. After that, the KLDA algorithm reduces the features' dimension. After that, the FLSL fuses the features, which are then inputted to the MDLNN. Centred on the generated rules, the person is classified as genuine or imposter by the MDLNN (explicitly, the features are trained and tested centred on that rule). Here, more hidden layers are employed in DL neural network, and the Stain Bowerbird Optimization (SBO) algorithm selects the optimal weight value for attaining higher accuracy. The proposed method's block diagram is exhibited in Figure 1,

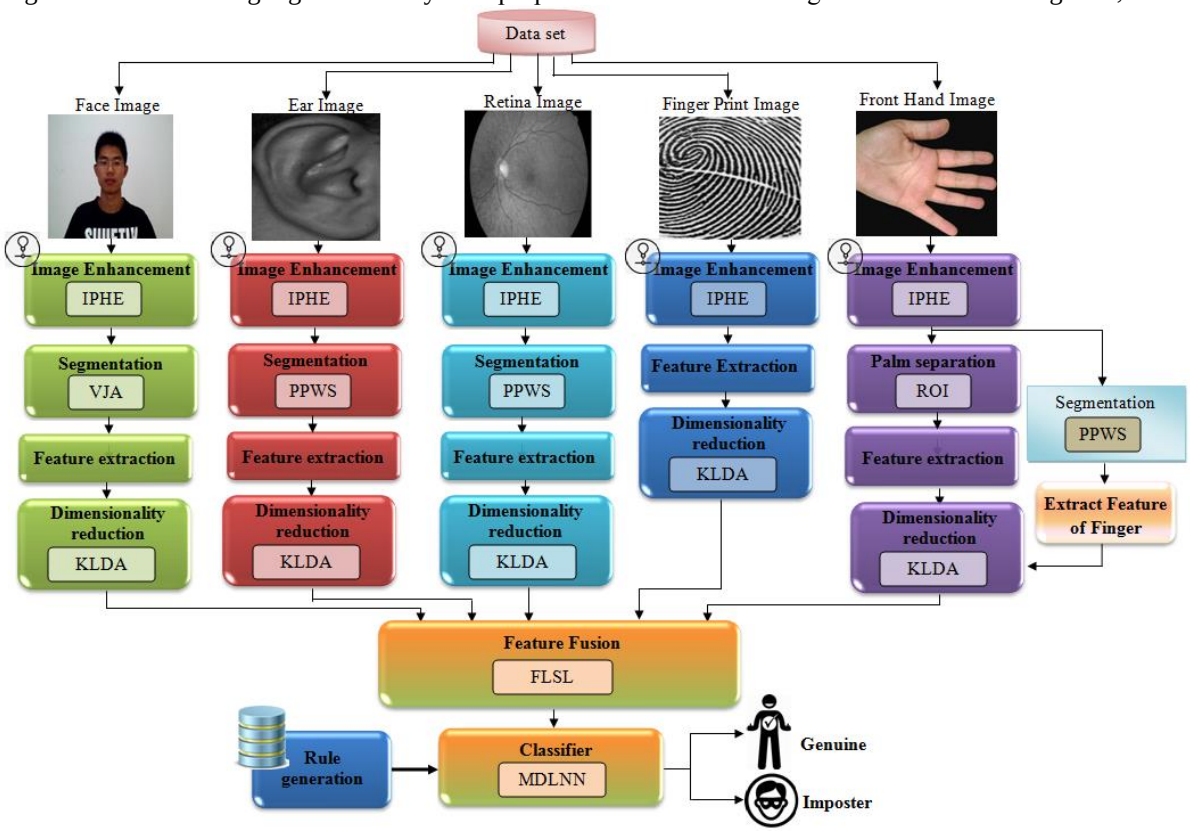

Figure 1: Block diagram for the proposed methodology

3.1 Image Enhancement

Initially, the IPHE algorithm enhances the input trait: face, ear, retina, finger-print, and front hand images. For the extraction of information as of the image, the image's contrast must be ameliorated. Over enhancement is a major issue for most contrast enhancement methods. Thus, the gamma correction function is considered here to evade that issue. The IPHE follows these steps: the images' pixel values are arranged (ascending order). Next, the histogram building will be generated, followed by which, the histogram median value is calculated, which is round of to the nearest integer value (i.e. threshold value). After that, the EXOR operations of equivalent '2' histogram values are performed and the values are considered as Cumulative Distributions Function (CDF). The image's histogram equalization is gauged as:

$$H_e = \frac{CDF}{A_p * N_o} \tag{1}$$

Wherein, H_e signifies the histogram equalization, A_p implies the entire number of pixels, N_o implies the number of output precise. At that moment, the over enhancement problem will occur. Thus, the gamma correction is employed to regulate the intensity that is rendered as,

$$M_{i(out)} = \omega M_{i(in)}^{\chi} \tag{2}$$

Wherein, $M_{i(in)}$ and $M_{i(out)}$ signify the input as well as output image intensities, correspondingly, ω and χ imply '2' parameters that control the transformation curve's shape.

3.2 Segmentation

Segmentation of traits, say, the face, ear, retina, finger, and palm is performed subsequent to image enhancement. Here, the VJA segments the face parts, and the PPWS algorithm takes care of the ear, finger (explicitly, unnecessary information elimination), and retina. In addition, via gauging the ROI, the palm is attained.

3.2.1 Face segmentation by VJA

VJA is robust and its face detection in practical situations is faster, thus it is preferred. Here, only the face parts (left and right eye, nose, lips, as well as eyebrows) are segmented. There are totally '4' section (i) Haar Features Selection, (ii) Generating an integral image, (iii) Adaboost Training, as well as (iv) Cascading.

Haar Feature Selection: Haar features are categorized into: a) '2'-rectangle features, which stands as the difference betwixt the sums of the pixels among '2' rectangular areas, b) '3'-rectangle features gauges the sum of pixels among '2' outside rectangles and is deducted as of the sum of pixels on the centre rectangle and c) '4' rectangle features gauges the difference betwixt the diagonal pairs of the rectangle.

Integral Image Computation: In the image, the integral image value of any point is equivalent to the sum of the entire pixels on the upper left corner of the point. The integral image at u, v encompasses the sum of the pixels above as well as to the left of u, v, inclusive:

$$in(u,v) = \sum_{u' \le u\ v' \le v} G_i(u', v') \tag{3}$$

Wherein, $in(u,v)$ signifies the integral image and also $G_i(u', v')$ implies the original image, $i = 1,2,....., n,$ the face image is signifies as G_1. The recursion formula is employed in the integral computation, which is described as,

$$cu(u,v) = cu(u, v-1) + G_i(u,v) \tag{4}$$

$$in(u,v) = in(u-1, v) + cu(u,v) \tag{5}$$

Wherein, $cu(u,v)$ signifies the cumulative row sum, the integral image can well be gauged on one pass above the image (original).

Adaboost Training: Adaboost algorithm eradicates redundant features and converts numerous features into a compact one. It stands as a learning classification function. Aimed at representing a face, the most meaningful ones are the chosen features. Several thousands of features can be lessened to a few hundred features by this algorithm.

Cascading: The cascaded classifier stands as a compilation of stages that encompasses a stronger classifier. Every phase verifies whether a specific sub-window is definitely not a face or maybe a face. If a specified phase classified a sub-window as a non-face, it will be discarded; whereas, if it is classified as a maybe face, it is sent to the succeeding stage on the cascade.

3.2.2 Palm separation

As of the improved front hand image, the palm's area is computed by computing the ROI region. The fingers are acquired separately in this computation. Extracting ROI is a necessary task. The ROI is computed

centred on the palm's rotation and also the region's size; consequently, the region's size is computed via the valleys' localization. The ROI's end result is articulated as,

$$ROI_{out} = \left(N - \frac{r_s}{2} \right) + 1 \tag{6}$$

Here, ROI_{out} signifies the ROI's outcome; N implies the novel rotation; r_s implies the novel region's size.

3.2.3 Ear, retina, and finger segmentation using PPWS

The occlusions, together with the other unwanted information (e.g., ear-rings, hair) are removed as of the improved ear image to acquire the actual ear region. The segmentation within the ear region is handled in the ear aimed at eradicating the redundant information. Next, the blood vessels are segmented to acquire the information in the retina's image. The segmentation procedure is implemented in the finger image aimed at the reason of eliminating unnecessary things prevalent in the image (for instance, some individual wears the rings such that the unnecessary things are eliminated). Herein, aimed at segmentation, the PPWS technique is utilized. The correlation calculation is executed in a typical watershed segmentation technique. However, it couldn't attain added information. Consequently, the Pearson correlation's computation is executed here; the over-segmentation issue is evaded via the penalty parameter. The morphological processes, like convolution, and also Pearson's correlation, are applied in this technique aimed at locating the foreground and also background detection. The convolution's arithmetic formulation is:

$$vol(G_i, k) = \sum_p \sum_q G_i \,.\, k(p, q) \tag{7}$$

Herein, vol signifies the convolution function; G_i implies the inputted image ($i = 1,2,.....,n,$; the ear and retina image is signified as G_2 and G_3; k symbolizes the kernel. Next, Pearson's correlation is computed. The correlation is nearly alike convolution. It is enumerated as the nearby pixels' weighted summation. The correlation is equated as,

$$rel(G_i, k) = \frac{n\sum_{p,q}(u+p)(v+q) - \left(\sum_p (u+p)\right)\left(\sum_q (v+q)\right)}{\sqrt{\left[n\sum_p (u+p)^2 - \left(\sum_p (u+p)\right)^2\right]\left[n\sum_q (v+q)^2 - \left(\sum_q (v+q)\right)^2\right]}} k(p,q) \tag{8}$$

Here, (u,v) implies the inputted image's pixel location; (p,q) signifies the actual image's pixel location.

3.3 Feature Extraction

The features are taken as of every trait past the segmentation and also palm separation. As of the segmented face parts, segmented retina's blood vessels, fingerprint, and also ear, the Local Tetra Pattern (LTrP), Gabor feature, edge, SURF, and also Binary Robust Invariant Scalable Key-points (BRISK) features are extracted. The minute points and also cross-line points are taken out as of the fingerprint utilizing these feature descriptors. The geometric features, LTrP, Discrete Wavelet Transform (DWT), and SIFT are extracted as of the palm. Next, the finger's geometric measurement is taken out as of every finger.

LTrP: The LTrP defines the local texture's spatial structure utilizing the central grey pixel's direction. t_c signifies the G_i image's central pixel; t_h implies t_c 's horizontal neighbour; t_v signify t_c 's vertical neighbour. Next, the 1st-order derivatives prevalent at the t_c is equated as,

$$G_{i(0^o)}^{(1)}(t_c) = G_i(t_h) - G_i(t_c) \tag{9}$$

$$G_{i(90^o)}^{(1)}(t_c) = G_i(t_v) - G_i(t_c) \tag{10}$$

Next, compute the pixels' magnitude $M_{G_i^1(t_p)}$ utilizing,

$$M_{G_i^1(t_p)} = \sqrt{\left(G_{i(0^o)}^{(1)}(t_p)\right)^2 + \left(G_{i(90^o)}^{(1)}(t_p)\right)^2} \tag{11}$$

Herein, t_p signifies the image's pixels.

Gabor Feature: A '2'-dimensional Gabor function is equated as,

$$ga(u,v)=\exp\left(-\frac{u'^2+v'^2}{2\sigma^2}\right)\cos\left(2\pi\frac{u'}{\lambda}+\varphi\right) \tag{12}$$

$$\begin{bmatrix}u'\\v'\end{bmatrix}=\begin{bmatrix}\cos\theta & \sin\theta\\-\sin\theta & \cos\theta\end{bmatrix}\begin{bmatrix}u\\v\end{bmatrix} \tag{13}$$

Here, $ga(u,v)$ signifies the Gabor result; $\lambda,\theta,\varphi,\sigma,u',v'$ are the wavelet's parameters.

SURF: SURF defines a local FE technique. It utilizes a local invariant fast key-point detector to take out the image's feature key points. It utilizes a unique descriptor to take the image's feature descriptor. SURF's features are in-variant of shifting, scaling and also rotation; it is partly invariant towards illumination and also affine transformation. Herein, the Hessian Matrix (HM) is found regarding the image G_i's each pixel position; it is arithmetically equated as,

$$H(u,\delta)=\begin{pmatrix}Z_{uu}(R,\delta) & Z_{uv}(R,\delta)\\Z_{uv}(R,\delta) & Z_{vv}(R,\delta)\end{pmatrix} \tag{14}$$

Here, R signifies the image's point; σ is signified as scale. Generally, $Z_{uu}(R,\sigma)$ implies the convolution of the image's Gaussian 2nd-order derivative at the respective point comprising the coordinates (u,v).

BRISK: BRISK is stated as a method aimed at scale-space Key-point's detection and also the binary description's creation. The Gauss function is utilized to decrement the grey-scale aliasing in the BRISK feature descriptor. The standard deviation sigma's Gauss function is proportional to the distance betwixt the points on every concentric circle. Picking a pair as of the point pairs created by every sampling point, signified as (L_m,L_n); the grey values past the treatment are $G_i(L_m,\rho_m)$ and also $G_i(L_n,\rho_n)$. Thus, the gradient betwixt '2' sampling points $gr(L_m,L_n)$ is,

$$gr(L_m,L_n)=(L_n-L_m).\frac{G_i(L_n,\rho_n)-G_i(L_m,\rho_m)}{\|L_n-L_m\|^2} \tag{15}$$

Split the pixel sets to '2' sub-sets: short separation pairs (Sh) and long-distance sets (Lo). Hence, the long, as well as short-distance pairs, are equated as,

$$Sh=\left\{(L_m,L_n)\in A\middle|\|L_n-L_m\|<\varepsilon_{\max}\right\}\subseteq A \tag{16}$$

$$Lo=\left\{(L_m,L_n)\in A\middle|\|L_n-L_m\|<\varepsilon_{\min}\right\}\subseteq A \tag{17}$$

Here, A signifies the compilation of all sampling points' pairs; $\varepsilon_{\max}$ and $\varepsilon_{\min}$ signifies the distance thresholds. Generally, the BRISK technique is utilized aimed at solving aimed at the overall pattern's direction gr regarding the gradient betwixt '2' sampling points:

$$gr=\begin{pmatrix}gr_u\\gr_v\end{pmatrix}=\frac{1}{Lo}.\sum gr(L_m,L_n).(L_m,L_n)\in Lo \tag{18}$$

Aimed at attaining scale as well as rotation invariance, the sampling pattern has been again sampled past the rotational angle $\theta=\arctan 2(gr_v,gr_u)$. The binary descriptor b_d's creation is executed by implementing eqn. (19) on all points' pairs prevalent in set Sh via the short-range sampling points.

$$b_d=\begin{cases}1 & G_i(L_n^\theta,\rho_n)>I(L_m^\theta,\rho_m)\\0 & otherwise\end{cases},\qquad \forall(L_m^\theta,L_n^\theta)\in Sh \tag{19}$$

Edge: Aimed at edge feature, the Canny edge's detection technique is employed. It comprises '5' stages: Smoothing, Finding the gradients, Non-maximal suppression, Thresholding, and then Edge tracking via hysteresis.

The smoothing stage eliminates the noise prevalent in the original image; the Gaussian filter is utilized aimed at this noise removal. After that, the sharpening alters the edge pixels detected by enumerating the image's gradient. The gradient signifies a unit vector that directs in the maximal intensity change's direction.

The gradient's vertical F_u as well as horizontal F_v components are calculated initially; next, the gradient's magnitude and the direction are enumerated; this calculation is executed at the finding gradients stage. The magnitude is enumerated as,

$$\theta = \arctan\left(\frac{|F_u|}{|F_v|}\right) \tag{20}$$

Just the local maxima are signified as edges in the 3rd step. Next, the potential and also the actual edges are specified via thresholding; this is executed at the thresholding phase. In the end step, the edges, which aren't connected to the strong edges, are suppressed.

DWT: The image's decomposition is executed utilizing the wavelet transform. The image has been disintegrating into '2' diverse frequency bands: LH, LL that comprises the horizontal contents and the approximate contents. The wavelet transform's definition is:

$$W_{t(di,tr)} = \int_{-\infty}^{+\infty} f(t)\,\frac{1}{\sqrt{di}}\,\psi * \left\{\frac{t-tr}{di}\right\} dt \tag{21}$$

Here, $W_{t(di,tr)}$ signifies the wavelet transform function; di, tr signify the dilation as well as the translation factors; $f(t)$ implies the wavelet transformation function; ψ implies the mother wavelet's dilation.

SIFT: The SIFT technique comprises '4' steps: (a) Scale-Space Extrema's Detection, (b) Key-point's Localization, (c) Orientation Assignment, and then (d) Key-point Descriptor's Generation. Scale-space functions are employed in the detection of the similar object's position as of the diverse dimensions. The scale-space function $r_g(u,v,\beta)$ is articulated as,

$$r_g(u,v,\beta) = Gau(u,v,\beta) * G_i(u,v) \tag{22}$$

Herein, $Gau(u,v,\beta)$ signifies the convolutional Gaussian function. The subsequent stage is the key-point localization that is the procedure of choosing the features section aimed at locating the formerly characterized. Every key point is allotted '1' or else more orientations centred on the local image's gradient directions in the orientation assignment stage. The end process is the Key-point Descriptor's generation that targets the main key-point descriptors' creation.

Geometric Features of Palm and fingers: The palm's and fingers' geometric features are taken out utilizing the Hough Transform function. The Hough transforms detecting a line that is articulated as,

$$d = u\cos\theta + v\sin\theta \tag{23}$$

Here, d signifies the distance as of the origin onto the nearby point on the straight line; θ implies the angle betwixt the u axis and the line linking the origin with the nearby point. The angle's measurement is as of the line to the fingers' rotation alongside the straight direction. Next, the fingers' width is enumerated in '3' diverse positions: in the finger's top, middle and then its bottom. The finger's 1st and end pixel are enumerated to compute the finger's width. The finger's length is partitioned to '3' segments (i.e.) top, middle and then final; after that, the width's measurement is as of the 1st pixel to the end pixel. Next, the palm region's height, width is enumerated by building the bounding box; the palm region's area is computed by utilizing the width and also the height. At last, the features taken out have been equated as,

$$B_f = a_i, \quad i = 1,2,.....,n \tag{24}$$

Here, B_f signifies the extracted feature's set; a_i implies the n-number of features.

3.4 Dimensionality Reduction by KLDA

As of the features taken out, necessary features are decremented utilizing the KLDA technique. As of every trait, the features are normalized utilizing Gaussian Kernel's function aimed at the cause of decrementing the errors in the classification stage; the Gaussian Kernel's function is articulated as,

$$\ker(u,v) = \exp\left(-\frac{\|u-v\|^2}{2\xi^2}\right) \tag{25}$$

Here, ξ implies the variable parameter. Past the feature dimension's normalization, the class matrix's mean vector is equated as:

$$\tau_i = \frac{1}{nn_j} \sum_{dd_i \in Dm_t} dd_i \tag{26}$$

Here, τ_i signifies the i^{th} feature's mean; dd_i implies the i^{th} sample; nn_j symbolizes the number of samples prevalent in the j^{th} feature; Dm_t signifies the data matrix. Next, identify all the features' total mean τ. Aimed at every sample of every class, the betwixt-class scatters' matrix bc_s and also the within-class scatters' matrix wc_s is equated as:

$$bc_s = \sum_{i=1}^{n} (\tau_i - \tau)(\tau_i - \tau)^{Tr} \tag{27}$$

$$wc_s = \sum_{i=1}^{n} \sum_{j=1}^{n_i} (Y_j - \tau_i)(Y_j - \tau_i)^{Tr} \tag{28}$$

Here, n signifies the number of training samples prevalent in the class i; τ_i implies the mean vector of samples originating as of class i; Y_j signifies that class's j^{th} data. wc_s implies the features' scatter about every class's mean; bc_s signifies the features' scatter about the overall mean aimed at every class.

3.5 Feature Fusion

Next, the Feature-level Fusion (FF), together with the Score-Level (SL) fusion is executed. Amidst all fusion techniques, this feature level technique aids in attaining maximal accuracy in-person identification. In FF , unwanted information can be prevalent in the features. The SL is computed aimed at decrementing the information as a single quantity. FF is identified via the easy concatenation of the feature's sets acquired as of the diverse traits. The concatenation procedure is equated as,

$$FF = \{a_i(G_1), a_i(G_2), a_i(G_3), a_i(G_4), a_i(G_5), a_i(G_6)\} \tag{29}$$

Here, $a_i(G_1), a_i(G_2), a_i(G_3), a_i(G_4), a_i(G_5), a_i(G_6)$ implies the facial, ear, retina, finger-print, fingers and also the palm features. After that, the SL computation is centred on score normalization that is vital to change the various systems' scores to a general domain prior to compiling them is provided as,

$$SL = \frac{S(a_i) - \min(S(a_i))}{\max(S(a_i)) - \min(S(a_i))} \tag{30}$$

Here, $S(a_i)$ signifies the features' original score values. Lastly, the end feature is signified as aa_i .

3.6 Rule Generation

The rules are created to test the template image past the feature reduction. The rule generation's combination is: i) every inputted trait is real signifying that the person is real, ii) every inputted trait is fake signifying that the person is the imposter, iii) '3' or else more than '3' inputted traits are fake signifying that the person is the imposter, and also iv) '1' or else '2' inputted traits are fake signifying that the individual is real.

3.7 Identification by using MDLNN

In this identification stage, the features extracted had been inputted into the MDLNN technique that finds the person regarding the rules generated. The technique comprises '3' layers. The 1st layer is the inputted layer (IL) and the final layer is the outputted layer (OL). Betwixt the IL and OL, extra layers of units may exist, termed Hidden Layers (HLs). n- number of HLs is pondered in this methodology. Hence, the NN comprises the accuracy issue owing to the weight updation process such that this study technique utilizes the Satin Bowerbird Optimization (SBO) technique aimed at HL's weight value selection. At first, the selected features' outputs are fed to the IL. The data as of the IL is inputted to the HL; in the HL, the hidden unit is enumerated aimed at the inputted features utilizing the eqn. (31):

$$hid_i = b_s + \sum_{i=1}^{n} aa_i . l_i \tag{31}$$

Here, b_s signifies the bias value; l_i implies the weight value; aa_i signifies the inputted features. Therefore, the HL's output is inputted to the OL. In the OL, the activation function is equated as,

$$ott_i = b_s + \sum_{i=1}^{n} hid_i . l_i \tag{32}$$

Here, ott_i signifies the outputted unit. Lastly, the loss function is enumerated utilizing the eqn. (33) as,

$$loss = (tar - ott_i) \tag{33}$$

Here, $loss$ signifies the loss function; ott_i implies the outputted unit; tar implies the network's targeted output. Past the loss computation, examine if the loss obtained matches with the particular threshold value; if it doesn't match then the weight value is optimized utilizing the SBO technique, otherwise the output is signified as the finalized output. Figure 2 exhibits the DLNN's pseudo-code,

Input: Outcome of Fused features aa_i
Output: Genuine (or) Imposter

Begin
Initialize neurons, input layer, hidden layer, output layer, weight value l_i, and loss threshold ll_t.
Calculate the hidden unit and output unit by,
$hid_t = b_s + \sum_{i=1}^{n} aa_i . l_i$ and $ott_t = b_s + \sum_{i=1}^{n} hid_t . l_i$
Check loss function
if $(loss \geq ll_t)$ {
Select the weight value of neurons by SBO
// Weight updation by SBO
Generate bowers
Evaluate fitness function
while the criteria is not satisfied **do**
Calculate the probability of bowers by, $pb_i = \frac{fit_i}{\sum_{n=1}^{N} fit_n}$
if $(co_i \geq 0)$ {
Calculate fitness function by, $\frac{1}{1+co_i}$
} **else** {
Calculate fitness function by, $1 + co_i$
}
end if
Change new position in each iteration
Calculate fitness function
Update elite if a bower becomes fitter than the elite
end while
} **else** {
Denote the output is the final output
}
end if
End

Figure 2: Pseudocode of MDLNN algorithm

The SBO technique comprises '5' stages: (a) random bowers generation, (b) probability calculation, (c) elitism, (d) position changes, and then (e) mutation.

(a) Random bowers generation: Initially, the set of bowers are created. The 1st population involves a sequence of positions aimed at bowers. Every position is determined as an n-dimensional vector of parameters. These values are initialized arbitrarily such that a uniform distribution is pondered betwixt the lower as well as upper limit parameters. The bower's attractiveness is specified by the compilation of parameters.

***(b) Probability calculation*:** Past initialization, aimed at every population members, the probability is computed. The male, together with the female satin bowerbird, choose the bower centred on the probability calculation. The probability function is enumerated as,

$$pb_i = \frac{fit_i}{\sum_{n=1}^{N} fit_n} \tag{34}$$

Here, pb_i signifies the probability function; N implies the total number of bowers; fit_i signifies the fitness function that is equated as,

$$fit_i = \begin{cases} \frac{1}{1+co_i} & co_i \geq 0 \\ 1+co_i & co_i < 0 \end{cases} \tag{35}$$

Here, co_i signifies the cost function's value in the i^{th} position or else i^{th} bower. The cost function is the function optimized by Eq. (35) that comprises '2' parts. The 1st part computes the final fitness in which values have been greater analogized to or equivalent to '0'; whilst the 2nd part computes the fitness aimed at values lesser than '0'. This eqn. comprises '2' main features.

(c) Elitism: Elitism permits the finest solution (solutions) to be conserved at each phase of the optimization procedure. The position of the best bower constructed by birds is proffered as the elite of iteration. The best individual in every iteration is conserved as the elite of iteration. Elites comprise the maximal fitness values and also it can affect other positions.

(d) Position changes: In every iteration, any bower's novel alterations can be enumerated as,

$$h_{ie}^{new} = h_{ie}^{old} + \nu_e \left(\left(\frac{h_{je} + h_{elite,e}}{2} \right) - h_{ie}^{old} \right) \tag{36}$$

Here, h_i signifies the i^{th} bower or else solution vector; h_{ie} implies this vector's e^{th} member; h_{ie}^{old} signifies the bower's old position; h_{ie}^{new} signifies the bower's new position; $h_{elite,e}$ implies the elite's position; h_{je} symbolizes the target solution amidst all the solutions prevalent in the present iteration; the parameter ν_e signifies the attraction power prevalent in the goal bower; it specifies the amount of step that is computed aimed at every variable. The ν_e is equated as,

$$fit_k = \frac{\nu}{1 + pb_j} \tag{37}$$

Here, ν implies the maximal step size; pb_j implies the probability attained by eqn. (34) utilizing the goal bower.

(e) Mutation: At every cycle's end, the random alterations are implemented with definite probability to prevent the male as of attacks, i.e., whilst the males have been busy constructing a bower upon the ground, other animals can attack them. The distribution and mutation procedure are articulated as,

$$h_{ie}^{new} \sim N_d \left(h_{ie}^{old}, \gamma^2 \right) \tag{38}$$

$$N_d \left(h_{ie}^{old}, \gamma^2 \right) = h_{ie}^{old} + \left(\gamma * N_d (0,1) \right) \tag{39}$$

Herein, N_d signifies the normal distribution; the γ implies the proportion of the space width and it is articulated as,

$$\gamma = d(\varepsilon) * \left(h(\text{var})_{\max} - h(\text{var})_{\min} \right) \tag{40}$$

Herein, $h(\text{var})_{\max}$ and $h(\text{var})_{\min}$ imply the upper and lower bound allotted to variables; the parameter $d(\varepsilon)$ implies the percentage difference betwixt the upper and lower bounds that is variable. All specified steps are continued till the fit_i is met. At last, the classifier categorised that the person is an imposter or else real centred on the created rule that is specified in the 3.5 section.

4. RESULT AND DISCUSSION

The proposed multi-biometric model's performance is examined. The proposed work is applied in MATLAB. The synthetic dataset is utilized by this work for the performance analysis. The dataset's sample images along with the further process of the image are displayed in Figure 3,

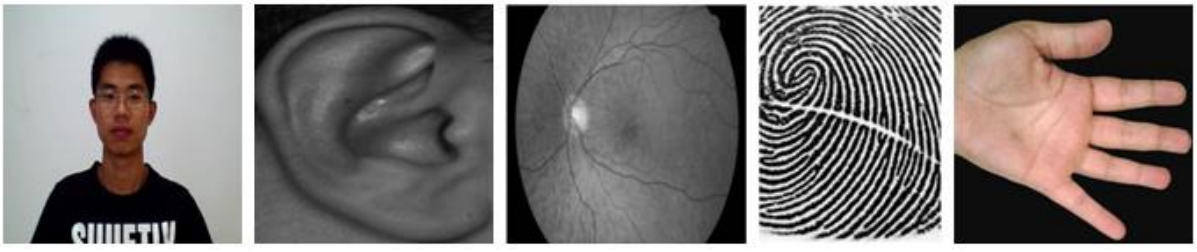

(a)

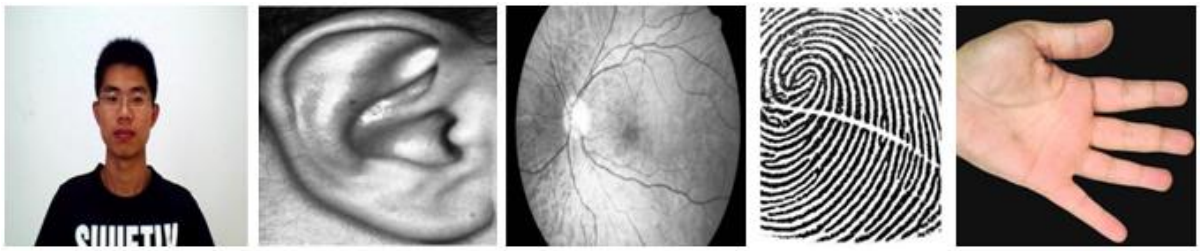

(b)

Figure 3: Sample images of all traits, (a) input image, and (b) enhanced image

The sample images of every trait, namely the face, ear, retina, fingerprint, along with front hand image are demonstrated in figure 3. Figure 3 (a) displays the dataset's input image and the enhanced image by utilizing the IPHE algorithm is displayed in figure 3 (b).

4.1 Performance analysis

The proposed MDLNN's performance is examined with the existent DL Neural Network (DLNN), Convolutional Deep Neural Networks (CDNN), along with Artificial Neural Networks (ANN) centered on sensitivity, specificity, accuracy, precision, recall, Negative Predictive Value (NPV), F-Measure, False Positives Rates (FPR), False Negative Rates (FNR), False Rejections Rate (FRR), False Discovery Rates (FDR), along with Matthews Correlations Co-efficient (MCC).

Table 1: Analysis of the performance of the proposed classifier with the existent classifiers based on sensitivity, specificity, and accuracy metrics

Performance Metrics	Proposed MDLNN	DLNN	CDNN	ANN
Sensitivity	0.9111	0.5887	0.2649	0.0056
Specificity	0.9555	0.7943	0.6324	0.8986
Accuracy	0.9407	0.7258	0.5099	0.6009

The MDLNN classifier's performance with the prevailing classifiers, namely DLNN, CDNN, and ANN, concerning sensitivity, specificity, along with accuracy metrics is established in Table 1. The ability to decide the persons rightly is sensitivity, the ability to determine the genuine persons rightly is specificity, and the accuracy metric is differentiating the persons and genuine cases correctly, which is indicated as the recognition rate. Now, the MDLNN algorithm's accuracy is 0.9407, the accuracy of the existent method is 0.7258 for DLNN, 0.5099 for CDNN, and 0.6009 for ANN. The CDNN achieves poor performance analogized to the prevailing methods along with the MDLNN centered upon the accuracy metric. Likewise, the proposed achieve a higher result, i.e. (0.9111) sensitivity, and (0.9555) specificity centered upon the other '2' metrics. The prevailing algorithms attain less performance analogized to the proposed work. It is inferred that the MDLNN centered MMB recognition system attains a better result analogized to the prevailing methods. The graphical depiction of table 1 is demonstrated in Figure 3,

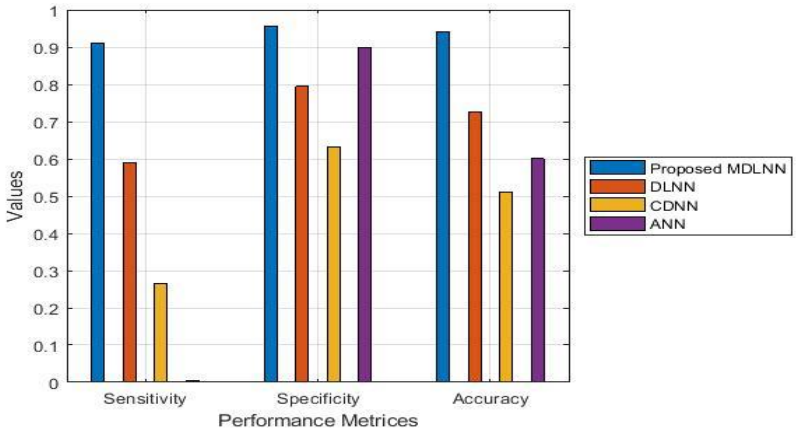

Figure 3: Analyze the performance of the proposed method with the existing methods based on sensitivity, specificity, and accuracy metrics

Table 2: illustrate the performance of the MDLNN classifier with the existing classifiers based on sensitivity, specificity, and accuracy metrics

Performance Metrics	Proposed MDLNN	DLNN	CDNN	ANN
Precision	0.9111	0.5887	0.2649	0.0268
Recall	0.9111	0.5887	0.2649	0.0056
F-Measure	0.9111	0.5887	0.2649	0.0092

Table 2 demonstrated the MDLNN classifier's performance with the DLNN, CDNN, along with ANN classifiers concerning the precision, recall, along with F-Measure metrics. The number of genuine class predictions is measured by the precision metric that belonged to the genuine class, recall measure specifies the total genuine class predictions made out of every genuine example in the dataset together with the amalgamation of both the precision along with recall metrics is the F-measure metric. The precision, recall, F-Measure value of the MDLNN classifier is 0.9111, and the existent methods have 0.5887 for DLNN, 0.2649 for CDNN, and the ANN has (0.0268) precision, (0.0056) recall, and (0.0092) F-Measure in this table 2. The existing ANN algorithm attains worst performance analogized to the existent techniques and also the proposed methods as concluded by this table. The existent DLNN algorithm is better than the CDNN and ANN but, it also gives lower performance than the proposed MDLNN. Therefore, it indicates that a better performance is achieved by means of the proposed MDLNN when contrasted to the prevailing research methods. The pictorial depiction of table 2 is exhibited in Figure 4,

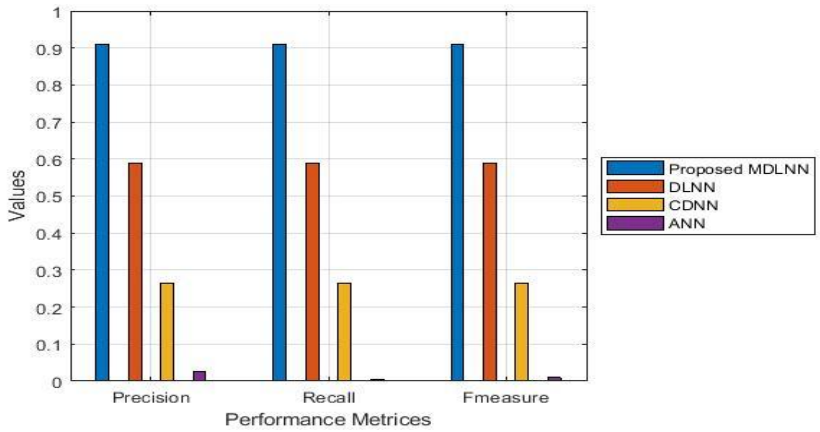

Figure 4: Comparative analysis of MDLNN with the other classifiers based on precision, recall, and F-Measure metrics

Table 3: Performance analysis based on NPV, FPR, and FNR

Performance Metrics	Proposed MDLNN	DLNN	CDNN	ANN
NPV	0.9555	0.7943	0.6324	0.6437
FPR	0.0444	0.2056	0.3675	0.1014
FNR	0.0888	0.4113	0.7350	0.9944

The performance metrics, NPV, FPR, and FNR centered analysis are done for the MDLNN with the prevailing classifiers in table 3. Now the first place is held by the MDLNN classifiers centered on NPV metric and hold the last place centered on FPR and FNR metric. The last place is held by the CDNN algorithm centered upon the NPV metric. The ANN holds first place and CDNN holds first place centered on the FPR metric. The NPV, FPR, and FNR value of the MDLNN is 0.9555, 0.0444, and 0.0888. The NPVE value of the CDNN is 0.6324. Overall, the proposed classifier has higher NPV as of the analysis and low FPR along with FNR result, therefore, it summarized that higher performance is acquired by the proposed MDLNN centered MMB recognition system analogized to the other method-centered recognition. The pictorial demonstration of table '3' is displayed in Figure 5,

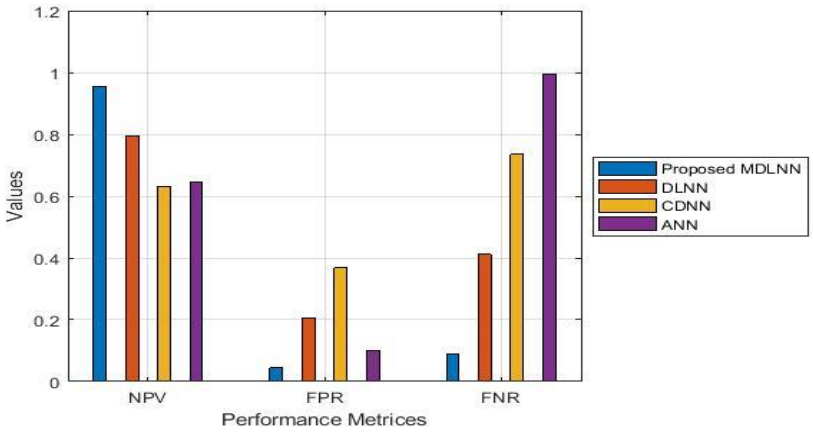

Figure 5: Performance analysis based on NPV, FPR, and FNR metrics

Table 4: Performance analysis based on NPV, FPR, and FNR

Performance Metrics	Proposed MDLNN	DLNN	CDNN	ANN
MCC	0.8667	0.3830	0.1025	0.1776
FRR	0.0888	0.4113	0.7350	0.9944
FDR	0.0888	0.4113	0.7350	0.9731

The proposed MDLNN classifier's performance with the existing DLNN, CDNN, and ANN algorithm concerning MCC, FRR, and FDR metrics is examined in Table 4. The true classes with the predicted classes are measured by the MCC, the FRR specifies the percentage of identification instances in which authorized persons are wrongly rejected, and the total false discoveries in recognition divided by means of the total discoveries in that recognition is FDR. Here, a higher MCC value i.e. 0.8667 is possessed by means of the proposed MDLNN algorithm along with lower FRR and FDR values. The CDNN and ANN possess lower MCC values and higher FRR and FDR values. The DLNN is much better as contrasted with the CDNN and ANN, but the DLNN also has low performance than the MDLNN. Therefore, better results are attained by the MDLNN in multi-biometric recognition. The graphical depiction of table 4 is exhibited in Figure 6,

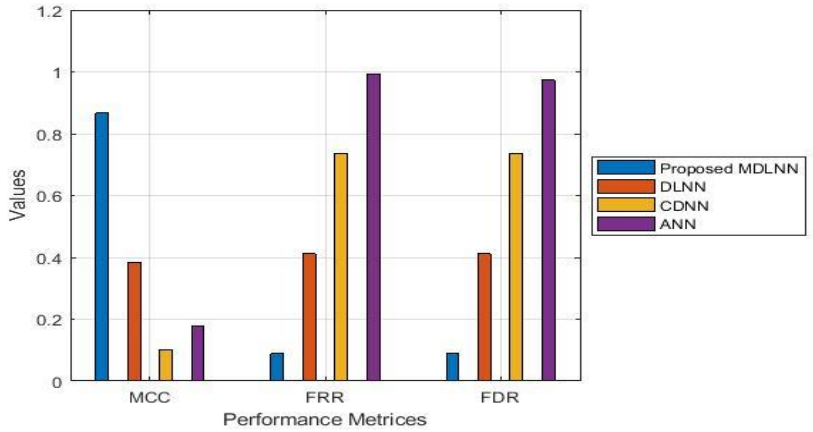

Figure 6: analyze the performance based on MCC, FRR, and FDR metrics

5. CONCLUSION

BR is stated as a budding technique and is attaining higher performance in recent years. This study method proffered an MMB recognition system centred on the FLSL fusion technique and also an MDLNN classifier. This methodology utilizes the face, iris, ear, fingerprint, and also front hand as the inputted traits. Herein, the MDLNN classifier is utilized to make the recognition system become more robust and also yields greater accuracy (also signified as the recognition rate). The synthetic dataset is acquired to examine the proposed multi-model BR system's performance, which is analogized with the existent DLNN, CDNN, and ANN techniques

regarding the accuracy, precision, recall, F-Measure, sensitivity, specificity, NPV, FPV, FNR, MCC, FRR, and also FDR. In this examination, the MDLNN proposed yields an efficient outcome analogized to the other classifiers centred on all performance metrics. The proposed MDLNN accuracy is (0.9407) that is greater analogized to every other classifier. Therefore, this research technique validated that the MDLNN proposed, segmentation and also enhancement centred multi-modal BR attains efficient outcomes analogized to the other techniques. This work can be improved in the upcoming future by implementing the latest technique to increment the performance and make the system more robust.

REFERENCES

1. Kumari P, "A fast feature selection technique in multi modal biometrics using cloud framework" , Microprocessors and Microsystems,vol. 79, pp. 103277,2020, 10.1016/j.micpro.2020.103277.
2. Sree Vidya B, and Chandra E., "Entropy based Local Binary Pattern (ELBP) feature extraction technique of multimodal biometrics as defence mechanism for cloud storage" , Alexandria Engineering Journal, vol. 58, no. 1, pp. 103-114 ,2019.
3. Basma Ammour, Larbi Boubchir, Toufik Bouden, and Messaoud Ramdani, "Face–iris multimodal biometric identification system" , Electronics vol. 9, no. 1, pp. 85, 2020.
4. Ibrahim Omara, Ahmed Hagag, Souleyman Chaib, Guangzhi Ma, Fathi E. Abd El-Samie, and Enmin Song, "A hybrid approach combining learning distance metric and dag support vector machine for multimodal biometric system" , IEEE Access 2020, 10.1016/j.micpro.2020.103277.
5. Milind E Rane, and Deshpande Prameya P, "Multimodal biometric recognition system using feature level fusion" , In International Conference on Computing Communication Control and Automation (ICCUBEA), IEEE, pp. 1-5, 2018, 10.1109/ICCUBEA.2018.8697821.
6. Haider Mehraj, and Ajaz Hussain Mir, "Feature vector extraction and optimisation for multimodal biometrics employing face, ear and gait utilising artificial neural networks" , International Journal of Cloud Computing, vol. 9, no. 2-3, pp. 131-149, 2020.
7. Gunasekaran Raja J K., and R. Pitchai, "Prognostic evaluation of multimodal biometric traits recognition based human face, finger print and iris images using ensembled SVM classifier" , Cluster Computing , vol. 22, no. 1, pp. 215-228, 2019.
8. Mohsen AM El-Bendary, Hany Kasban, Ayman Haggag, and M. A. R. El-Tokhy, "Investigating of nodes and personal authentications utilizing multimodal biometrics for medical application of WBANs security" , Multimedia Tools and Applications,vol.79, no. 33, pp. 24507-24535, 2020.
9. Shaveta Dargan, and Munish Kumar, "A comprehensive survey on the biometric recognition systems based on physiological and behavioral modalities" , Expert Systems with Applications vol. 143, pp. 113114, 2020.
10. Swati K Choudhary, and Ameya K. Naik, "Multimodal Biometric Authentication with Secured Templates—A Review", In International Conference on Trends in Electronics and Informatics (ICOEI), IEEE, pp. 1062-1069, 2019, 10.1109/ICOEI.2019.8862563.
11. Aman Kathed, Sami Azam, Bharanidharan Shanmugam, Asif Karim, Kheng Cher Yeo, Friso De Boer and Mirjam Jonkman, "An enhanced 3-tier multimodal biometric authentication", In International Conference on Computer Communication and Informatics (ICCCI),IEEE, pp. 1-6, 2019, 10.1109/ICCCI.2019.8822117.
12. Rachid Chlaoua, Abdallah Meraoumia, Kamal Eddine Aiadi and Maarouf Korichi, "Deep learning for finger-knuckle-print identification system based on PCANet and SVM classifier", Evolving Systems, vol. 10, no. 2, pp. 261-272, 2019.
13. Karthiga R and MangaiS,"Feature selection using multi-objective modified genetic algorithm in multimodal biometric system", Journal of Medical Systems, vol. 43, no. 7, pp. 1-11, 2019.
14. YanTong, Frederick W. Wheeler and Xiaoming Liu, "Improving biometric identification through quality-based face and fingerprint biometric fusion", In IEEE Computer Society Conference on Computer Vision and Pattern Recognition-Workshops, pp. 53-60, 2010, 10.1109/CVPRW.2010.5543233.
15. Annamalai Prakash R. Krishnaveni and Ranganayakulu Dhanalakshmi, "Continuous user authentication using multimodal biometric traits with optimal feature level fusion", International Journal of Biomedical Engineering and Technology, vol. 34, no. 1, pp. 1-19, 2020.
16. El mehdi Cherrat, Rachid Alaoui and Hassane Bouzahir, "A multimodal biometric identification system based on cascade advanced of fingerprint fingervein and face images", Indonesian Journal of Electrical Engineering and Computer Science, vol. 18, no. 1, pp. 1562-1570, 2020.
17. Gayatri U Bokade and Rajendra D. Kanphade, "Secure Multimodal Biometric Authentication Using Face, Palmprint and Ear a Feature Level Fusion Approach", In International Conference on Computing, Communication and Networking Technologies (ICCCNT),IEEE, pp. 1-5, 2019, 10.1109/ICCCNT45670.2019.8944755.

18. Mohammad Haghighat, Mohamed Abdel-Mottaleb and Wadee Alhalabi, "Discriminant correlation analysis: Real-time feature level fusion for multimodal biometric recognition", IEEE Transactions on Information Forensics and Security, vol. 11, no. 9, pp. 1984-1996, 2016.
19. Karthiga Rand MangaiS,"Feature selection using multi-objective modified genetic algorithm in multimodal biometric system", Journal of Medical Systems, vol. 43, no. 7 pp. 1-11, 2019.
20. Nada Alay and Heyam H. Al-Baity, "deep learning approach for multimodal biometric recognition system based on fusion of iris, face, and finger vein traits", Sensors, vol. 20, no. 19, pp. 5523, 2020.
21. Meryem Regouid, Mohamed Touahria, Mohamed Benouis and Nicholas Costen, "Multimodal biometric system for ECG, ear and iris recognition based on local descriptors", Multimedia Tools and Applications, vol. 78, no. 16, pp. 22509-22535, 2019.
22. Gurjit Singh Walia, Tarandeep Singh, Kuldeep Singh and Neelam Verma, "Robust multimodal biometric system based on optimal score level fusion model", Expert Systems with Applications, vol. 116, pp. 364-37, 2019, 10.1016/j.eswa.2018.08.036.
23. Prabu S, LakshmananM and V. Noor Mohammed, "A multimodal authentication for biometric recognition system using intelligent hybrid fusion techniques", Journal of Medical Systems, vol. 43, no. 8, pp. 1-9, 2019.
24. Gaurav Jaswal, Amit Kaul and Ravinder Nath, "Multimodal biometric authentication system using hand shape palm print and hand geometry", In Computational Intelligence Theories Applications and Future Directions-Volume II,Springer, Singapore, pp. 557-570, 2019, 10.1007/978-981-13-1135-2_42.
25. Gunasekaran K, RajaJ and R. Pitchai, "Deep multimodal biometric recognition using contourlet derivative weighted rank fusion with human face fingerprint and iris images", Automatika Časopis Za Automatiku Mjerenje Elektroniku Računarstvo I Komunikacije, vol. 60, no. 3, pp. 253-265, 2019.